Preparation and Characterization of $Ba_{0.6}K_{0.4}BiO_3$ Nano Particles with High Visible Light Photo Catalytic Activity

K. Sharma*, S. Jain and U. Chandrawat

Department of Chemistry, Govt. P.G.College, Kota 324001, India

ABSTRACT

Herein, we report the synthesis of a novel nano-structured photo catalyst $Ba_{0.6}K_{0.4}BiO_3$ by Pechini method. Prepared catalyst is characterized using simultaneous thermogravimetric differential thermal analysis (TG–DTA), ray diffraction (XRD), Scanning electron microscopy (SEM), Ultra Violet Diffuse reflectance spectroscopy (UV-DRS) and Fourier-transform infrared spectroscopy (FT-IR). The XRD pattern suggests that $Ba_{0.6}K_{0.4}BiO_3$ crystallizes in the cubic structure. The formation of perovskite phase can be confirmed by the presence of metal-oxygen band in the FTIR spectrum. SEM image reveals the nano sized plate like structure of $Ba_{0.6}K_{0.4}BiO_3$ with particle size in the range of 10-45 nm. The band gap is calculated from the DRS and is found to be 1.8eV. The band gap and crystalline nature suggest that this material can be used as a photo catalyst. The photo catalytic activity of $Ba_{0.6}K_{0.4}BiO_3$ is evaluated for degradation of Malachite Green dye under visible light irradiation. The results reveal that 0.75 gL^{-1} $Ba_{0.6}K_{0.4}BiO_3$ with initial concentration of Malachite Green 40 mgL^{-1} irradiated for 30 minutes shows the highest photo catalytic activity. According to Langmuir-Hinshelwood kinetic model, the photo catalytic degradation of Malachite green dye follows pseudo-first-order kinetics.

INTRODUCTION

Today, the top global issues are concerned with ensuring a clean environment and a sustainable supply of clean energy at reasonable cost. For these reasons many researchers are studying advanced materials and processes for the removal of waste or photocatalytic cracking of toxic wastes efficiently at low cost and with less energy consumption and advanced materials. These processes for the production of clean and renewable energy are used for photocatalytic and photoelectrocatalytic water splitting, and also the photocatalytic reduction of organic waste material.

Malachite green chloride (*N*-[4-[[4-(dimethylamino) phenyl]phenylmethylene]-2,5-cyclohexadien-1-ylidene]-*N*-methylmethaminium chloride, is a triphenyl methane dye worldwide used in aquaculture. It is extensively used as biocide in the global aquaculture industry, and is highly effective against important protozoan and fungal infections. It is also used as a food colouring agent, food additive, medical disinfectant and anthelminthic as well as a dye in the silk, wool, jute, leather, cotton, paper and acrylic industries [1-2]. The US Food and Drug Administration has nominated malachite green (MG) as a priority chemical for carcinogenicity test. There is a concern about the fate of MG and its reduced form, leucomalachite green in aquatic and terrestrial ecosystem science, as they occur as contaminants and are potential human health hazards [3-4]. Considering the potential adverse effects of MG, it should be removed from the environment. Although the use of MG has been banned in several countries; it is still being used in many parts of the world due to some benefits like low cost, ready availability and appreciable efficacy. Photocatalytic degradation of dyes and organic pollutants is of fundamental importance in waste water treatment and other related problems of environmental interest. Recently many new perovskite-based semiconductor materials are being used as visible-light-active photocatalysts [5-6]. Several features associated with oxygen deficiency like band gap energy, cation vacancy and surface area influence the performance of

* Corresponding author: K. Sharma
E-mail: kavi21089.sharma@gmail.com; Tel- +919461391230

material used in photo catalytic degradation. When semiconductor is irradiated with the photons whose energy is greater than or equal to the band gap energy of the semiconductor; the hole-electron pairs are generated. These hole-electron pairs are responsible for generation of other reactive oxidising species like O_2^-, $HOO°$, HOO^-, $HO°$ etc. which further react with adsorbed dye molecule, leading to the formation of dye radical anions and finally the degradation of the dye occurs [7-8].

The perovskite type oxides ABO_3 own special physical and chemical features because of their stable crystal structure, electromagnetic behaviour, magneto resistive properties and high catalytic activity. They have been applied in environmental protection and industrial catalysis [9-10]. Most of the metal cations are known to be stably incorporated in the perovskite structure. One of the major characteristics of perovskites is the possibility for substitutions at the position of cations. As a result, there are large groups of compounds with different cations in A position $\{A_yA'_{1-y}BO_3\}$ [11-12] and with different cations in B position $\{AB_yB'_{1-y}O_3\}$ [13-14] and with substitution in positions of both the cations $\{A_xA'_{1-x}B_yB'_{1-y}O_3\}$ [15-16]. Potassium doped $BaBiO_3$ perovskite semiconductor material was discovered by Mattheiss et al. in 1988 [17]. Conventionally, potassium doped $BaBiO_3$ powders have been prepared by a traditional solid state reaction [18] and powder sintering technique [19] which needs high temperature and may lead to the presence of impure phases like Bi_2O_3 in the prepared catalyst [18]. In order to overcome these disadvantages, we used Pechini method (sol-gel technique) [20] which is simple and economical, low processing temperature and wide range of possibility to change the properties by varying the composition of the solution [21].

In the present study, $Ba_{0.6}K_{0.4}BiO_3$ nano structured material is prepared by Pechini method and the structural properties of $Ba_{0.6}K_{0.4}BiO_3$ are examined by various characterization techniques. The photo catalytic activity of thus prepared material is evaluated by the degradation of MG using Langmuir-Hinshelwood kinetic model [22-23]. To the best of our knowledge $Ba_{0.6}K_{0.4}BiO_3$ has never been used as a photo catalyst.

MATERIAL AND METHODS

Materials

Barium nitrate, bismuth nitrate, potassium nitrate, citric acid and ethylene glycol are purchased from Merck (India). The MG dye is purchased from SDS Fine Chem. (P) Ltd., India. Deionised water further purified with a milli-Q-water ion exchange system (Millipore Co.) is used throughout the study. Chemical structure of MG dye is shown in Fig. 1. All chemicals are of analytical grade and are used as received.
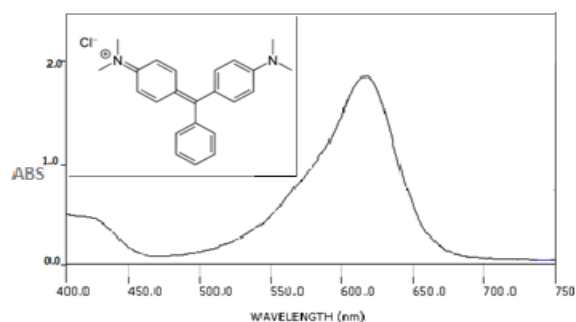

Figure 1. Molecular structure of Malachite Green dye ($\lambda_{max}=620nm$).

Preparation of $Ba_{0.6}K_{0.4}BiO_3$ perovskite

Pechini method,[20] which is used to prepare mixed metal oxide powders, it is used here to synthesize $Ba_{0.6}K_{0.4}BiO_3$. This process is based on metallic citrate polymerization with the use of ethylene glycol. A hydro carboxylic acid (such as citric acid), is used to chelate cations in aqueous solution. Polymerization is promoted by heating the mixture, and it results in the formation of homogeneous resin in which metal ions are uniformly distributed.[21] There are some complicating factors experienced during other conventional methods some of which have been discussed in our previous research work.[24,25] In the present study, for the preparation of $Ba_{0.6}K_{0.4}BiO_3$ particles, barium nitrate, potassium nitrate and bismuth nitrate are used as starting materials. Atomic ratio of barium nitrate, potassium nitrate and bismuth nitrate is 3:2:5. First, barium nitrate and potassium nitrate are dissolved in deionised water under stirring condition. Bismuth nitrate is separately dissolved in minimum amount of dilute HNO_3 to avoid precipitation of Bi ions; then, it is added dropwise to the barium nitrate and potassium nitrate solution. Citric acid is then added proportionally to the above metal solution, followed by the addition of ethylene glycol as a chelating agent. The citric acid/ethylene glycol ratio is kept at 3:2. The solution thus prepared, while being stirred with a magnetic stirrer, is heated up to 90°C to remove excess water and subsequently to accelerate poly esterification reaction between citric acid and ethylene glycol. During the evaporation of solvent, reddish brown gas corresponding to NO_2 comes out of the solution. This produces a viscous, bubbly mass that forms a resin upon cooling. This precursor is burned at 350°C for 2 hours. Further, to fully evaporate highly combustion species in the mass and to burn down most of the organic constituents, the powder is calcined in a furnace at different temperatures (6 hours at 650°C and 12 hours at 720°C). The calcination removes most of the residual carbon and thus cubic phase perovskite is finally obtained. Experimental conditions for catalyst loading $0.75gL^{-1}$, pH 5.5 (natural pH), absorbance is recorded at

λ_{Max}= 620 nm, light intensity 137 mWcm^{-2}, continuous stirring, temperature 35°C.

Characterization

To determine the best calcination temperature, simultaneous thermogravimetric (TG) and differential thermoanalytic (DTA) measurements are achieved in flowing air (200mL/Min.) with heating rate of 5°C/min upto 900 °C using a Netzsch STA449 system. The structural characterization is done by X-ray diffraction using a X-ray diffractrometer [Siemens D500] equipped with a high intensity CuKα radiation, and operated at 45kV and 40mA accelerating voltage and the applied current, respectively. A scan rate of 5°/min was used for 0°-90° two-theta values. The morphology and particle size are analyzed using Scanning electron microscope [HitachiX650, Japan]. Fourier transform infrared (FTIR) [Spectrum 100, Perkin Elmer] is utilized to identify chemical bonds existing in the powder. UV-DRS spectra is carried out using Schimadzu Lambda 900 spectrophotometer. The spectra is recorded at 240-800 nm wavelength.

Photocatalytic activity

The photocatalytic degradation is performed using a cylindrical glass reactor, accommodating a central glass tube in which an 500W Xe arc lamp (intensity=137mWcm^{-2}) is placed to irradiate the dye solution. At the bottom of the reactor, a magnetic stirrer is placed for homogenization of reaction solution. The visible light illumination is started following a dark period (without light illumination) of 15 minutes to attain an adsorption equilibrium between dye and photocatalyst. Blank experiment (without $Ba_{0.6}K_{0.4}BiO_3$ photocatalyst) is also carried out. The samples are collected at regular time interval and subsequently analyzed for the residual concentration using a UV-VIS spectrophotometer at the wavelength of 620nm. Finally, the photocatalytic activities are determined using the following relation:

$$Degradation\ \% = Co - Ct/\,Co \qquad (1)$$

where, C_o (mgL^{-1}) and C (mgL^{-1}) are the initial concentration and concentration after photocatalytic degradation, respectively. A series of experiments are carried out to study the effect of the amount of photocatalyst and initial dye concentration on the photocatalytic degradation of MG dye at natural pH (5.5) and 35°C temperature.

RESULTS AND DISCUSSION

Simultaneous TG and DTA investigations are carried out to evaluate the crystallization temperature. Fig. 2 shows DTA-TGA curve of polymeric resin for $Ba_{0.6}K_{0.4}BiO_3$

indicating evolution of perovskite phase with increasing temperature. TGA curve shows a four step decomposition of resin precursor to form the perovskite material. We observed a slight weight loss of ~ 6% upto 200°C accompanied by a weak exothermic peak at 190°C. This weight loss is caused by elimination of residual water adsorbed due to the storage of the preheated sample in ambient atmosphere. The second weight loss region (42%) is observed in the range of 210-300°C is because of combustion of light organic matter and acetates as indicated by an exothermic peak around 240°C in DTA curve. The third weight loss around 23% in the temperature range of 310-580°C corresponds to decomposition of the nitrates and nitrites residue. This observation is supported by the well resolved exothermic peak at 550°C in DTA curve. The final small weight loss on the TGA curve observed above 560°C to 900°C corresponds to the crystallization and formation of perovskite phase (at 720°C) which is also confirmed by XRD (Fig. 3) and FTIR (Fig. 4) analysis. The total weight loss of this powder is 72.51%.
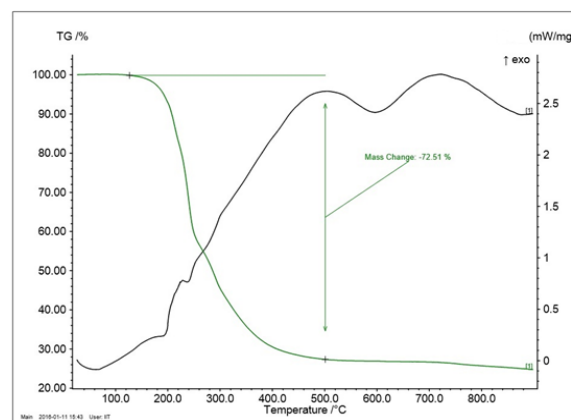

Figure 2. TGA/DTA curves showing thermal decomposition of precursor to a stable $Ba_{0.6}K_{0.4}BiO_3$.

Fig. 3 shows the XRD patterns of the $Ba_{0.6}K_{0.4}BiO_3$ compound. The patterns reveal that the sample burned at 350°C is amorphous in nature. Upon calcination at 650°C the sample becomes more crystalline (inset of Fig. 3). The sample calcined at 720°C is highly crystalline with predominantly perovskite structure. Though, its JCPDS card is not available, it could be seen that the diffraction peaks can be well indexed to cubic phase $Ba_{0.6}K_{0.4}BiO_3$ (pm3m space group and lattice parameter of 4.284Å) which are in accordance with the earlier studies reported by Flemming et al. [18]. In the Fig. 3 main diffraction peaks are observed at 20.53°, 29.33°, 36.66°,42.74°, 51.33°, 60.41°,68.280°, 76.04°and 83.37° which can be assigned to 100, 110, 111,200, 201, 220, 310 and 321 planes, respectively. Diffraction peak related to Bi_2O_3 are not observed in XRD pattern confirming the purity of the synthesized compound.
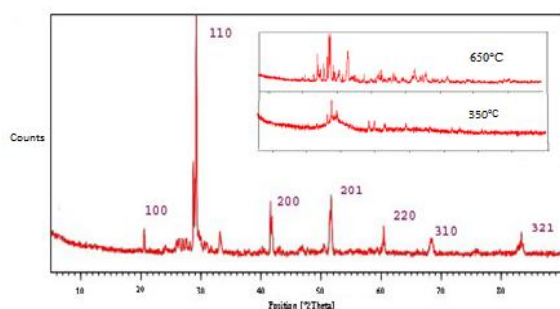
Figure 3. XRD pattern of $Ba_{0.6}K_{0.4}BiO_3$ calcined at 720°C for 12h. The inset shows the XRD pattern of precalcined samples.

Fig. 4 shows the FTIR spectra of $Ba_{0.6}K_{0.4}BiO_3$. The band at nearly $465cm^{-1}$ is related to Bi-O bending mode vibrations. The strong peak at $615cm^{-1}$ is related to anisotropic oxygen motions, which depends on the potassium ion distribution in the crystal lattice [26]. For the Pechini method, as ethylene glycol is used for polyesterification with citric acid to form a rigid polymer network, a strong band around $1105cm^{-1}$ is attributed to the C-C-O structure confirming the polymerisation process [27]. The FTIR results thus confirms that complex formation between citric acid and metallic ions occurred in the sol-gel route and that polyesterification of ethylene glycol and citric acid and complexation with metallic ions occurred in the Pechini Method. It is seen from the Fig. 2 that the peak at $1425cm^{-1}$ is attributed to Ba-O bending vibrations [28]. Thus, the bands at $615cm^{-1}$ and $1425cm^{-1}$ are due to creation of new active sites in the photocatalyst, which results in the higher activity of $Ba_{0.6}K_{0.4}BiO_3$ photocatalyst.
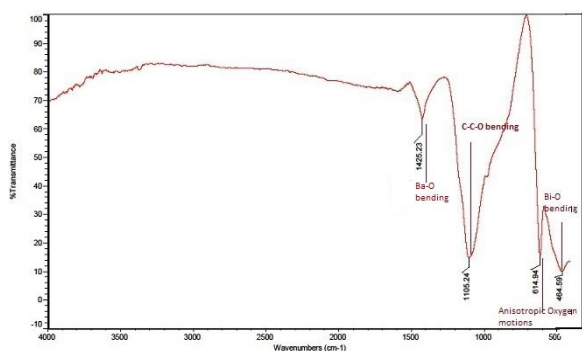

Figure 4. FTIR spectra for $Ba_{0.6}K_{0.4}BiO_3$.

As shown in Fig. 5 the prepared $Ba_{0.6}K_{0.4}BiO_3$ sample is sensitive to visible light and can absorb a wide range of light irradiation up to maximum 663 nm, almost covering the region from UV through all strong visible light under indoor lamp irradiation. This indicates that the prepared $Ba_{0.6}K_{0.4}BiO_3$ sample can be utilized as visible light active catalyst for degrading the dye pollutants. The band edge calculations verifying the

oxidative potential of prepared photocatalyst done by using $E=hc/\lambda$ where h, c and λ are Planks constant (Joule-sec), speed of light (meter/sec) and cut of wavelength (meters) respectively. During the band gap energy calculations $1eV=1.6\times10^{-19}$ joules are taken as conversion factor. The optical band is estimated to be 1.87eV, which is in good agreement with reported value [29] of 1.4eV for cubic $Ba_{0.6}K_{0.4}BiO_3$.

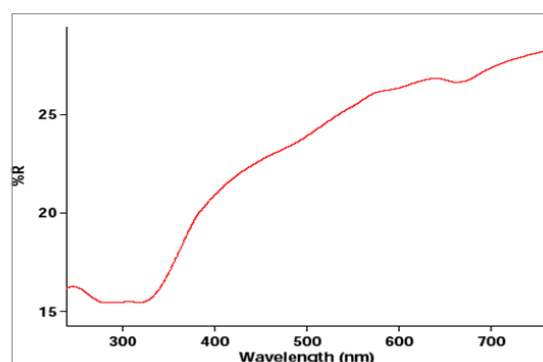**Figure 5.** UV-vis diffuse reflectance spectra of $Ba_{0.6}K_{0.4}BiO_3$.

Fig. 6 is the SEM micrograph of $Ba_{0.6}K_{0.4}BiO_3$ powder as prepared at 720°C. SEM shows well packed plate-like layered grains of variable sizes. The layered plate-like morphology is a characteristic feature of the bismuth containing compounds [30]. The encircled area in Fig. 4 shows weakly bound agglomeration process, which is attributed to Vander-Waals forces. In order to reduce the surface energy, the primary particles tend to form agglomerates with a minimum surface to volume ratio. This type of structure is common in oxides, ferrites, and titanate ceramics prepared by sol gel procedure [22,31]. The nanoparticles have an average size in the range of 45-101 nm

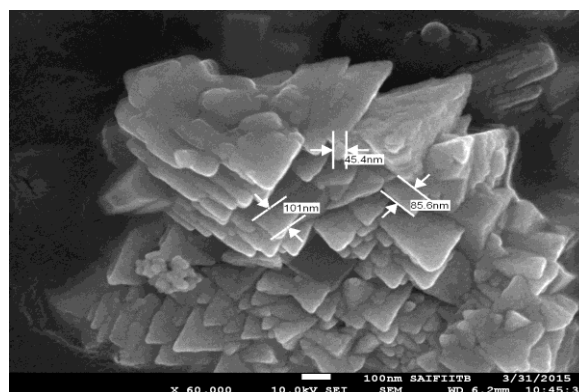**Figure 6.** SEM micrograph of $Ba_{0.6}K_{0.4}BiO_3$

The effect of initial concentration of dye on degradation rate can be determined by varying the initial concentration from 20 mgL^{-1} to 60 mgL^{-1} at constant

catalyst loading (0.75gL^{-1}). As seen in Fig. 7, degradation efficiency increases with increase in the dye concentration up to 40 mgL^{-1} after this the degradation efficiency decreases. This effect can be explained as follows; as the dye concentration increased, more molecules of dye are available for excitation and degradation. Above optimum concentration, the dye starts acting like a filter for the incident light. Considering the Beer-Lambert law, at higher concentration of dye, the path length of photons entering the solution decreases, resulting in the lower photon adsorption on catalyst particles and consequently, lowering the photo degradation rate. The observation is consistent with previous studies done by Chen *et al.* [5, 32-33].
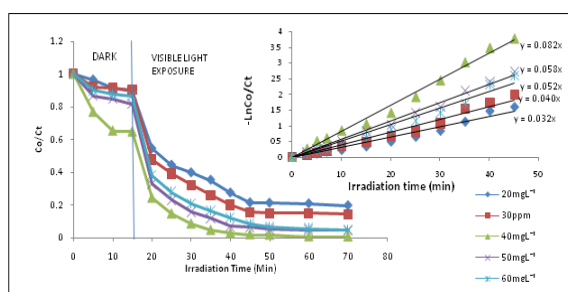

Figure 7. Effect of initial dye concentration on photochemical degradation of MG following dark adsorption with Ba$_{0.6}$K$_{0.4}$BiO$_3$ under visible light irradiation. Inset shows the plot of –LnC$_0$/C$_t$ versus irradiation time.

From both mechanistic and application point of view, studying the dependence of the photocatalytic reaction rate on amount of the Ba$_{0.6}$K$_{0.4}$BiO$_3$ in the MG dye degradation is important. Hence, the effect of photocatalyst concentration on the photodegradation rate of the MG dye is studied by varying the catalyst loading from 0.5gL^{-1} to 1.0gL^{-1} with initial dye concentration 40mgL^{-1}. As shown in Fig. 8, dye degradation is faster for catalyst dose of 0.75gL^{-1} than 0.5gL^{-1} and 1.0gL^{-1}. At lower catalyst loading number of active site are lesser so, initially when the amount of catalyst increases, the number of active sites increase which further increases the degradation rate. After exceeding the optimal catalyst loading, the suspended catalyst reduces the penetration of the light in the solution and decrease in the rate of photocatalytic degradation of dye is observed.

The overall rate of the photocatalytic degradation can be represented as R=R$_1$+R$_2$, where R, R$_1$and R$_2$ are net degradation, rate of photolysis and rate of photo catalysis, respectively. Though, it should be noted that no dye degradation is observed in the blank experiments, this reveals that there is a negligible effect with the visible light alone. Accordingly, the decrease in the

concentration of dye is due to the effect of both the catalyst and visible light [34].
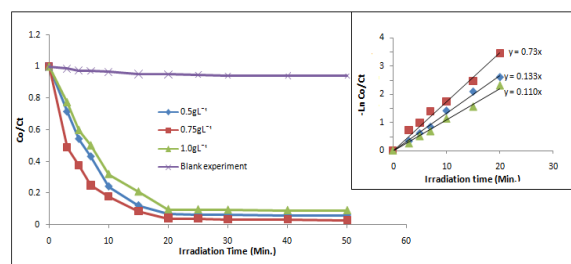

Figure 8. Influence of the catalyst concentration on the photodegradation of MG. Inset shows the plot of –LnCt/Co versus irradiation time.

Heterogeneous photo catalysis process, takes place over the catalyst surface. Therefore, reactant adsorption on catalyst surface is regarded as an important initial process. Fig. 7 also shows adsorption of MG on Ba$_{0.6}$K$_{0.4}$BiO$_3$ surface as a function of time. The result indicates that concentration of MG is decreased by 3%. The concentration of the dye after the 15 minutes dark adsorption is taken as the initial concentration (C$_o$).

The photocatalytic degradation of MG dye on the surface of Ba$_{0.6}$K$_{0.4}$BiO$_3$ nanoparticles follows a pseudo-first-order kinetic law and can be expressed by equation

$$LnCo/Ct = Kapp * t \qquad (2)$$

The curves of - LnC$_o$/C$_t$ against 't' are recorded and fitted linearly; the value of pseudo-first order rate constant (K$_{app}$) is extracted from the slope of the straight line (inset of Fig. 7). Thus obtained K$_{app.}$ is multiplied by respective initial dye concentration to calculate initial reaction rate (R$_o$).According to numerous works, the kinetics of the photocatalytic degradation is described by using the Langmuir-Hinshelwood (LH) model [22-23].
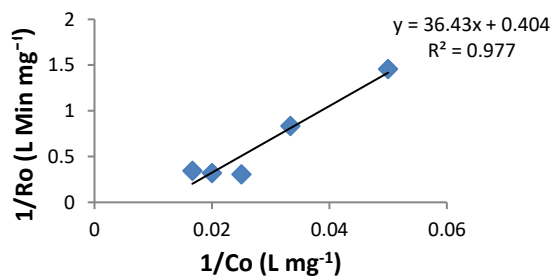

Figure 9. Langmuir-Hinshelwood plot of visible light degradation of MG in Ba$_{0.6}$K$_{0.4}$BiO$_3$ suspension.

The linear form of LH model is given by the following expression:

$$1/Ro = 1/kr + 1/kr. KLH. Co \qquad (3)$$

here, k_r and K_{LH} are the reaction rate constant and adsorption constant (Langmuir-Hinshelwood constant), respectively. Fig. 9 shows the graph between R_o^{-1} and C_o^{-1}, giving a straight line, with a slope of $(k_r.K_{LH})^{-1}$ and intercept of k_r^{-1}. k_r and K_{LH} values are 0.011 $mgL^{-1}min^{-1}$, 2.475 Lmg^{-1}, respectively.

CONCLUSION

$Ba_{0.6}K_{0.4}BiO_3$ nanostructured powder is prepared by Pechini method. The X-ray pattern indicates the cubic structure for the prepared catalyst. SEM image of calcined powder shows plate like nanostructured grain in range of 45-101 nm. The diffuse reflectance spectrum shows that the catalyst has a broad absorbance around 663nm with band gap of 1.8eV. Due to the low band gap, the catalyst is tested for the photo catalytic activity in the visible light exposure. The study confirms that the degradation of MG dye can be achieved by photo catalysis in the presence of an aqueous suspension of $Ba_{0.6}K_{0.4}BiO_3$. The degradation process is strongly influenced by the initial dye concentration and catalyst dose. The best degradation results are obtained at catalyst loading 0.75gL^1 and initial concentration of the dye solution of 40mgL^{-1} at natural pH (5.5) and 35°C temperature. Moreover, degradation kinetics of MG dye can be well described by Langmuir-Hinshelwood model and this process follows pseudo-first-order kinetics. Finally, it is concluded that the $Ba_{0.6}K_{0.4}BiO_3$ nanoparticle can be utilized as photo catalyst for the degradation of wastewater containing dyes and other organic compounds.

Acknowledgements

REFERENCES

1. Schnick, R. A. 1988. The Impetus to Register New Therapeutants for Aquaculture. The Progressive Fish-Culturist, 50(4): 190-196.
2. Culp, S. J., F. A. Beland, 1996. Malachite green: a Toxicological Review. Journal of the American College of Toxicology, 15: 219-238.
3. Rao, K. V. K., 1995. Inhibition of DNA Synthesis in Primary Rat Hepatocyte Cultures by Malachite Green: a New Liver Tumor Promoter. Toxicology Letters, 81 (2-3), 107-113.
4. Nelson, C. R., R. A. Hites, 1980. Aromatic Amines in and Near the Buffalo River. Environmental Science and Technology, 14:147-149.
5. Chen, C. C.; C. S. Lu, Y. C. Chung, J. L. Jan, 2007. UV Light Induced Photodegradation of Malachite Green on TiO2 Nanoparticles. Journal of Hazardous Material, 141: 520-528.
6. Kako, T., Z. Zou, M. Katagiri, J. Ye, 2007. Decomposition of Organic Compounds Over NaBiO3 Under Visible Light Irradiation. Journal of Hazardous Materials, 19: 98-202.
7. Tang, J., Z. Zou, Y. Jinhu , 2007. Efficient Photocatalysis on BaBiO3 Driven by Visible Light. Journal of Physical Chemistry C, 111(34): 12779-12785.
8. Yu, K., S. Yang, C. Liu, H. Chen, H. Li, C. Sun and S. A. Boyd, 2012. Degradation of Organic Dyes via Bismuth Silver Oxide Initiated Direct Oxidation Coupled with Sodium Bismuthates Based Visible Light Photo Catalysis. Environmental Science and Technolology, 46, 7318-7326.
9. Dong, B., Z. Li, Z. Li, X. Xu, M. Song, W. Zheng, C. Weng, S. S. A. Deyab, M. E. Newehy, 2010. Highly Efficient LaCoO3 Nanofibers Catalysts for Photocatalytic Degradation of Rhodamine B. Journal of American Ceramic Society. 93: 3587-3590.
10. Gupta, R. K., I. J. Choi, Y. S. Cho, H. L. Lee, S. H. Hyun, 2008. Characterization of Perovskite-Type Cathode, La0.75Sr0.25Mn0.95-xCoxNi0.05O3+d (0.1≤X≤0.3), for Intermediate-Temperature Solid Oxide Fuel Cells. Journal of Power Sources. 187: 371-327.
11. Kumar, K. V., K. Porkodi, A. Selvaganapathi, 2007. Heterogeneous Photocatalytic Decomposition of Crystal Violet in UV Illuminated Sol-Gel Derived Nanocrystalline TiO2 Suspension. Dyes And Pigment, 75: 246-249.
12. Lemos, F. C. D., E. Longo, E. R. Leite, D. M. A Melo, A. O. Silva, 2004. Synthesis of nanocrystalline Ytterbium Modified PbTiO3. Journal of Solid State Chemistry. 177: 1542-1548.
13. Alemi, A., E. Karimpour, H. Shokri, 2008. Preparation, Characterization and Luminescent Properties of Europium Oxide Doped Nano LaMn0.9Zn0.1O3+d by Sol-gel Processing. Bulletin of Material Science, 31: 967-973.
14. Lou Y., X. Li, X. Liu, 2009. NTCR Behaviour of La-doped BaBiO3 Ceramics. Advances in Material Science and Engineering. 383842: 1-4.
15. Shao, J., Y. Tao, J. Wang, C. Xu, W. G. Wang, 2009. Investigations of Precursors in the Preparation of Nanostuctured La0.6Sr0.4Co0.2Fe0.8O3-$ Via a Modified Combined Complexing Method. Journal of Alloy and Compounds. 484: 263-267.
16. Kaur, A., A. Singh, A. Asokan, L. Singh, 2014. Structural and Optical Properties of Iron Doped Barium Strontium Titanate. International Journal of Education and Applied Research, 4: 26-28 .
17. Mattheiss, L. F., D. R. Hamann, 1988. Electronic Structure of the High-Tc Superconductor Ba1-xKxBiO3. Physical Review Letters, 60:2681-2684.
18. Flemming, R. M., P. Marsh, R. J. Cava, J. J. Krajewski, 1988. Temperature Dependence of the Lattice Parameters in the 30-K Superconductor Ba0.6K0.4BiO3 . Physical Review B, 38:7026-7028.
19. Kim, H. G., D. W. Hwang and J. S. Lee, 2004. An Undoped, Single-phase Oxide Photocatalyst Working Under Visible Light. Jornal of American Chemical Society, 126: 8912-8913.
20. Pechini, M. U. S. Patent No. 3.330.697 (11 July 1967).
21. Fernandes, J. D. G., D. M. A. Melo, L. B. Zinner, C. M. Sulustiano, Z. R. Silva, A. E. Martinelli, M. Cerqueira, C. A. Junior, E. Longo, M. I. B. Bernardi, 2002. Low-Temperature Synthesis of Single-Phase Crystalline LaNiO3 Perovskite via Pechini Method. Materials Letters. 53: 122-125.
22. Kumar, K. V., K. Porkodi, A. Selvaganapathi, 2007. Heterogeneous Photocatalytic Decomposition of Crystal Violet in UV Illuminated Sol-Gel Derived Nanocrystalline TiO2 Suspension. Dyes and Pigment. 75: 246-249.
23. Kumar, K. V., K. Porkodi, F. Rocha, 2008. Langmuir–Hinshelwood Kinetics – A Theoretical Study. 9: 82-84.
24. Jain, S., K. Sharma, U. Chandrawat, 2014. Low-Temperature Synthesis, Characterization and Photocatalytic Activity of Nanorods BaBio3 Perovskite under Visible Light Irradiation. International Journal of Innovative Research in Science, Engineering Tecnology. 3:14405-14411.
25. Jain, S., K. Sharma, U. Chandrawat, 2016. Photocatalytic Degradation of Anti-Inflammatory Drug on Ti Doped BaBiO3

Nanocatalyst Under Visible Light Irradiation. Iranica Journal of Energy and Environmental. 7 (1): 64-71.

26. Lee, C. Y., K. Y. Song and R. P. Sperline, 1996. Molecular Dynamics Simulation and Far Infrared Measurements of Ba0.6K0.4BiO3. Korean Journal of Materials Research, 6(6): 555-560.

27. Gupta, M., P. Yadav, W. Khan, A. Azam, A. H. Naqvi, R. K. Kotlana, R.K. 2012. Low Temperature Synthesis and Magneto Resistance Study of Nano La1-xSrxMnO3 (x= 0.3, 0.33 and 0.4). Advanced Materials Letters, 3:220-225.

28. Legesse, F., K. Sreenu, S. Kena, K. Legesse, 2015. Synthesis and Characterization of BaBiO3 Perovskite Through Chemical Route. Science Technology and Arts Research, 4:80- 83.

29. Jung, D., E. Choi, 1999. Differences of Structural and Electronic Properties in Ba1-xKxBiO3 (x= 0, 0.04 and 0.4). Bulletin of Korean Chemical Society, 20:1045-1048.

30. Martín-González, M.S., J. García-Jaca, E. Moran, M. Á. Alario-Franco, 1998. Synthesis of BaBiO3 and Ba1-xKxBiO3 Films via an Electrodeposition Processes. Physica C, 297:185-191.

31. Marcos, F. R., J. J. Romero, J. F. Fernandez, 2012. Effect of the Temperature on the Synthesis of (K, Na)NbO3-Modified Nanoparticles by a Solid State Reaction Route. Journal of Nanoparticle Research, 12: 2495-2502.

32. Simões, A. Z., E. C. Aguiar, A. H. M. Gonzalez, J. Andrés, E. Longo, J. A. Varela, 2008. Strain Behaviour of Lanthanum Modified BiFeO3 Thin Films prepared via Soft Chemical Method. Journal of Applied Physics, 104:104115-1-1041156-6.

33. Alahiane, S., S. Qourzal, M. E. Ouardi, A. Abaamrane, A. Assabbane, 2014. Factors Influencing the Photocatalytic Degradation of Reactive Yellow 145 by TiO2-Coated Non-Woven Fibers. American Journal of Analytical Chemistry, 5:445-454.

34. Zhang, D., 2012. Heterogeneous Photocatalytic Removal and Reaction Kinetics of Rhodamine-B Dye With Au Loaded TiO2 Nanohybrid Catalyst. Polish Journal of Chemical Technology, 14: 42-48.

Persian Abstract

چکیده

در این تحقیق سنتز یک نانو ذره جدید به عنوان فتو کاتالیست با استفاده از روش پچینی مورد مطالعه قرار گرفت. کاتالیست تولید شده با استفاده از XRD، TGA، SEM، UV-DRS و FT-IR مورد بررسی قرار گرفت. آنالیز XRD ساختمان کریستالی کاتالیست تولیدی را اثبات کرد. سایز نانو ذره تولیدی با استفاده از آنالیز SEM 45 نانومتر تعیین شد. مقدار ۱/۸ الکترون ولت به عنوان فاصله پیوند تعیین شد. خواص نانو ذره در از بین بردن مالاشیت سبز مورد بررسی قرار گرفت.